# SHOCK ATTENUATION OF INTERVERTEBRAL DISC FOLLOWING FATIGUE LOADING

**C.-K. Chiang** [*] **C.-L. Yang** [**] **W.-C. Chen** [*] **C.-H. Chang** [*]

*Institute of Biomedical Engineering*
*National Taiwan University*
*Taipei, Taiwan 10617, R.O.C.*

**S.-C. Huang** [***]

*Department of Mechanical Engineering*
*National Taiwan University of Science and Technology*
*Taipei, Taiwan 10607, R.O.C.*

**J.-L. Wang** [****]

*Institute of Biomedical Engineering*
*National Taiwan University*
*Taipei, Taiwan 10617, R.O.C.*

## ABSTRACT

Shock absorption is one of the fundamental biomechanical functions of disc. The knowledge of the effect of fatigue loading, impact energy and contact period on the disc shock attenuation is important in clarifying the risk factors of back pain and evaluating the efficacy of novel disc prosthesis. The purpose of this study is to find the changes of shock attenuation of motion segment after fatigue loading, and the effect of impact energy and contact period on the disc shock attenuation pre and post fatigue loading.

The 3-unit porcine spinal motion segment was used for testing. The impact test was applied pre and post fatigue loading. Impact energy and contact period were controlled in the experiment. Shock attenuation properties, including the acceleration attenuation (AA) of disc, force transmissibility (FT) and phase delay of force (PDF) of motion segment, were calculated from the acceleration and force responses.

The results showed that the shock attenuation properties (acceleration attenuation and force transmissibility) decreased post fatigue. The disc acceleration attenuation was independent of impact energy and contact period. The disc acceleration attenuation was 0.78 (–1.06dB) pre fatigue and 1.04 (0.14dB) post fatigue. The force transmissibility of motion segment decreased post fatigue only during short contact period. The phase delay of force did not change significantly post fatigue.

We found that the fatigue loading decreased the disc shock attenuation. The disc was at higher risk of injury following fatigue loading even at a mild impact loading. The disc acceleration attenuation was invariant of impact energy and contact period, but decreased post fatigue. The disc acceleration attenuation is a good index to evaluate the degree of fatigue injury.

**Keywords :** Intervertebral disc, Impact loading, Fatigue, Acceleration attenuation, Force transmissibility, Phase delay of force.

## 1. INTRODUCTION

Epidemiological studies suggested highly repetitive activities as a risk factor for low back pain (LBP) [1,2]. Occupations that require higher cumulative spinal compression and shear forces often led to LBP problems [3]. The fatigue loading encountered due to exposure to whole body vibration (WBV) has also been pointed out as a risk factor for occupational low back disorders [4,5]. Moreover, combined shock and WBV constituted a critical detrimental factor for spinal health [6-8]. However, the safe limits of repetitive activities, WBV and shocks that prevent spinal disease are not reliably confirmed. Relations between disc function and fatigue loading are not understood clearly.

Shock absorption is one of the fundamental biome-

[*] Undergraduate student [**] Graduate student [***] Professor [****] Professor, corresponding author



DOI : 10.1017/jmech.2011.2

Copyright © 2011 The Society of Theoretical and Applied Mechanics, R.O.C.
https://doi.org/10.1017/jmech.2011.2 Published online by Cambridge University Press

chanical functions of disc. The disc is a viscoelastic structure consisting of a nucleus pulposus (NP) surrounded by anulus fibrosus (AF). The AF is an elastic laminated fibrous structure that holds the intradiscal pressure, hence providing the capability of shock absorption [9]. The micro failure of AF due to fatigue loading is expected to damage the shock absorption capability of disc. However, the quantitative links between fatigue loading and shock attenuation is inadequately studied.

To address these questions, this paper aims to investigate the shock attenuation of motion segment following fatigue loading. The effect of impact energy and contact period on the disc shock attenuation pre and post fatigue was analyzed. The shock attenuation was evaluated by the capability of acceleration attenuation (AA) of disc, force transmissibility (FT) and phase delay of force (PDF) of motion segment. Quantitative information of the effect of fatigue, impact energy and contact period on shock attenuation is important for defining the potential injury of disc and the efficacy of novel disc prosthesis [10-12].

## 2. MATERIAL AND METHOD

### 2.1 Specimen Preparation

Thirteen fresh 3-unit-motion-segment spine specimens (T2/T5 and T6/T9) from 6-month old swine were obtained immediately following death. The specimens were stripped of all soft tissue except all ligamentous, capsular, and intra-capsular structures were preserved. The disc and facet joints were also remained intact. The specimens were mounted at both ends, *i.e.*, the proximal half of cranial vertebra and the distal half of caudal vertebra, using quick setting epoxy. The specimens were placed in double plastic bags and frozen at −20°C for storage. Before experiments, the specimens were removed from freezer and kept in room temperature for 6 hours. The specimens were wrapped with gauze and saline during the experiments to keep the specimen's moisture. All discs used were rated grade 1 according to criteria defined by Galante [13] (Fig. 1). The size of tested disc was close to the size of human thoracic disc [14,15] (Table 1).

### 2.2 Impact Testing Apparatus and Acceleration Measurement

A "drop-tower type" testing apparatus was used for impact testing (Fig. 2). The impact energy was generated by the free fall of impactor and was transmitted to the specimen through the impounder. The shock absorber was placed on the top of the impounder to control the impact contact period. The contact period is the time interval that impactor compresses the impounder before it bounces back. Two types of shock absorbers were designed to provide the 20 ms and 40 ms contact time [16]. The specimen was mounted vertically below the impounder with a uni- axial load cell (Kistler 9021A, Kistler Instrumente, Winterthur, Switzerland) and above the six-axial force load cell

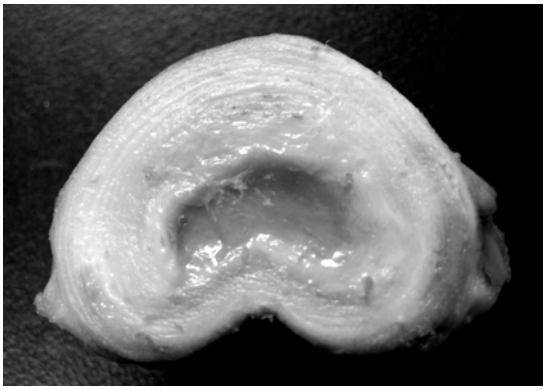


Fig. 1 The porcine thoracic disc

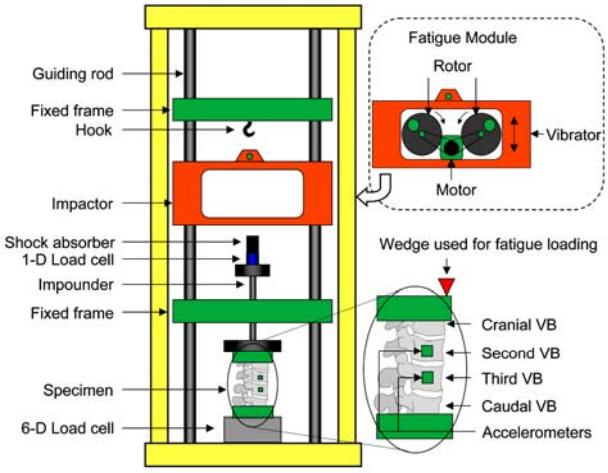



Fig. 2 Impact testing apparatus, fatigue testing module and placement of accelerometers. The impact energy, generated by the free fall of the impactor, was transmitted to the specimen through impounder. The fatigue loading, generated by the vibration of vibrator, was also transmitted to the specimen through impounder. The two accelerometers were placed on the surface of second and third vertebral body

Table 1 Dimensions (mm) of Porcine and Human Discs

| | Porcine thoracic disc | Human thoracic disc |
|---|---|---|
| Disc height | 5.2 (0.3) | *6.6 (1.4) |
| Disc width | 34.1 (2.4) | **EPWu = 28.6 (4.7), EPWl = 31.0 (5.3) |
| Disc depth | 22.5 (0.9) | **EPDu = 26.2 (4.6), EPDl = 27.3 (4.4) |

Data are Average (standard deviation).
* [14]
** Data are based on the measurement of endplate. [15]
EPWu: Upper endplate width, EPWl: Lower endplate width,
EPDu: Upper endplate depth, EPDl: Lower endplate depth,

(AMTI MC6-6-4000, Advanced Mechanical Technology, Inc., Watertown, MA, USA). The signal from the uni-axial load cell was defined as the "input force". The signal from the six-axial force load cell was defined as the "output force". Both the input and output forces were the resultant forces due to impact



https://doi.org/10.1017/jmech.2011.2 Published online by Cambridge University Press

energy. Two accelerometers (ADXL250EB, Analog Device Inc., USA) were attached on the second and third vertebral body (VB) to detect the vertical vibration/acceleration (Fig. 2). We used a high-speed 64-channel acquisition card (PCI-6071E, National Instrument, Inc., Austin, TX, USA) to record the signals of two accelerometers, input forces, output forces and moments. Half seconds data were recorded at 10 kHz sampling rate. The signals were low-pass filtered at 500 Hz frequency using Butterworth filtering algorithm.

### 2.3 Fatigue Loading Apparatus

A vibrator composed of two eccentric rotors and one motor was mounted into the impactor of the impact testing apparatus to create a vertical fatigue loading. The fatigue loading was produced by the rotation of two counter-rotated eccentric rotors driven by a motor. The vibration was transmitted to the specimen through the impounder. The specimen was vertically loaded on top of the anterolateral site of specimen using an eccentric wedge, approximately 4cm from the center of vertebrae, to mimic the combination of axial compression and lateral flexion (Fig. 2) [17]. The root mean squared averaged axial loading of cyclic loading was 425N (670N maximum and 270N minimum). The loading frequency was 5Hz and the loading time was 5 hours. In total, 90,000 loading cycles were applied.

### 2.4 Experimental Protocol and Data Analysis

Two specimens were used to confirm the morphological changes post fatigue by MR T1-Weighted-Image (T1WI) and cross-sectional dissected disc photography. Eleven 3-unit-motion-segment specimens were tested. The independent variables include contact period (short vs. long contact time, *i.e.*, 20 ms vs. 40 ms), impact energy (3.6 J, 6.0 J, 8.4 J, generated by loading height: 30, 50, 70mm, loading weight: 12kg) and fatigue loading (pre and post fatigue). The dependent variables include AA, FT and PDF.

The curve of the acceleration is sinusoid-like during an impact period. In the beginning, the acceleration is negative (VB moved downward and contact force increased). After the contact force reached its maximum, the acceleration is positive (VB moved upward and contact force decreased) (Fig. 3). The magnitudes of peak-to-peak acceleration (*i.e.*, the difference between the minimum and maximum acceleration) of the second and third VB during the impact period were collected.

The AA of disc is defined by the following equation:

$$\text{Acceleration Attenuation } (AA) = G_3/G_2 \qquad (1)$$

where the $G3$ is the peak-to-peak acceleration of third VB, and $G2$ is the peak-to-peak acceleration of second VB during the impact period.

The FT of motion segment is defined by the following equation:

$$\text{Force Transmissibility } (FT) = F_{\text{Max}.output} / F_{\text{Max}.input} \qquad (2)$$

where the $F_{\text{Max}}$ input is the maximum input force measured above the specimen, and the $F_{\text{Max}}$ output is the maximum output force measured beneath the specimen.

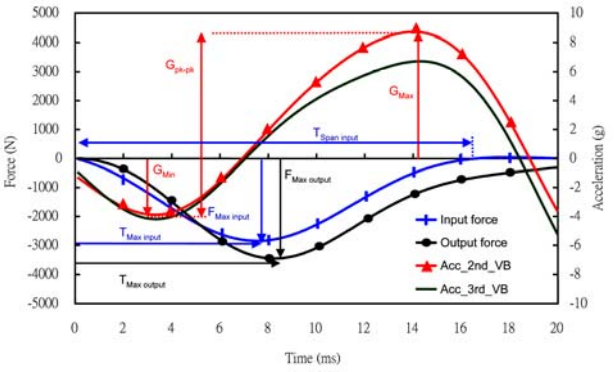



Fig. 3 A typical force and acceleration response of a 20 milliseconds impact. The input force is the force measured above the specimen, and output force is the force measured beneath the specimen

The PDF of output force with respect to the input force is calculated using the following equations:

$$\text{Phase Delay of Force } (PDF) = (T_{\text{Max}.output} - T_{\text{Max}.input}) / T_{Span.input} \times 100\% \qquad (3)$$

where the $T_{\text{Max}.output}$ is the time from start to the maximum output force, the $T_{\text{Max}.input}$ is the time from start to maximum input force, and the $T_{Span.input}$ is the time span, *i.e.*, the contact period, of input force.

### 2.5 Statistical Analysis

The paired-sample *t*-test was used to detect the statistical difference of AA, FT and PDF between pre and post fatigue loading. One-way analysis of variance (ANOVA) was used to detect the statistical differences of the AA, FT and PDF in the effect of contact period, impact energy at pre and post fatigue. All tests were considered to be significant at $\alpha = 0.05$. The analysis for this paper was generated using SAS Learning Edition 4.1 software (SAS Inst Inc, Cary, NC, USA).

## 3. RESULTS

### 3.1 Morphological Observation

No visible protrusion of NP was observed post fatigue. For the assuring of the injury post fatigue, a solution of black ink dye was injected into the center of the discs before fatigue loading. After the fatigue loading, the photography of cross-sectional dissected disc showed the NP protruded to the posterolateral side that was similar to the clinical observation of herniated intervertebral disc (Fig. 4). The lamellae of AF was distorted and the level of disc injury corresponded to stage 2 injury based on the criteria proposed by Adams and Hutton [18]. The MR T1WI also showed the thinning of AF and shortening of disc (Fig. 5).

### 3.2 Acceleration Attenuation (AA)

The magnitude of minimum, maximum, and peak-to-peak accelerations of second VB decreased post fatigue.



https://doi.org/10.1017/jmech.2011.2 Published online by Cambridge University Press



Fig. 4 Photograph of a sectioned disc post fatigue load. After axial loading combine with left anterolateral flexion fatigue loading, the nucleus pulposus protruded toward the right posterolateral side of the disc

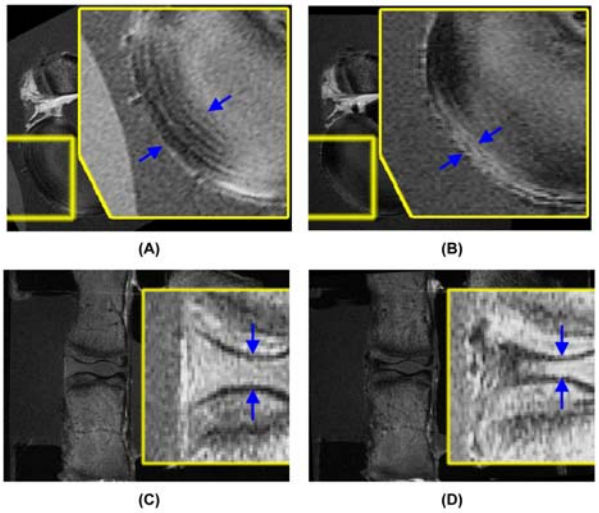



Fig. 5 The MR T1-Weighted-Images (T1WI) of spine pre fatigue (A, C) and post fatigue (B, D). The anulus fibrosus was thinning, and the disc was shortening post fatigue loading. The (A, B) are the cross-sectioned images, and (C, D) are the sagittal-sectioned images

The accelerations increased with impact energy but decreased with contact period pre and post fatigue (Table 2A). The average AA was 0.78 pre fatigue loading, and increased to 1.04 post fatigue loading. The AA was independent of impact energy and contact period pre and post fatigue loading (Table 2B).

### 3.3 Force Transmissibility (FT)

Only the maximum input force during short contact loading increased post fatigue. The maximum input and output forces increased with impact energy but decreased with contact period at pre and post fatigue (Table 3A). The FT during short contact loading decreased post fatigue. The FT during long contact loading did not change post fatigue. The FT decreased with impact energy during short contact loading at pre and post fatigue. The FT also decreased with contact period at pre and post fatigue (Table 3B).

Table 2A The Outcomes of the Accelerations of Minimum, Maximum and Peak-To-Peak of Second and Third Vertebral Body Pre and Post Fatigue at Different Levels of Contact Period and Impact Energy

| | | | | $G_{Min}$ (g) | | | $G_{Max}$ (g) | | | $G_{pk-pk}$ (g) | |
|---|---|---|---|---|---|---|---|---|---|---|---|
| | | *Energy* | Pre fatigue | Post fatigue | P-value | Pre fatigue | Post fatigue | P-value | Pre fatigue | Post fatigue | P-value |
| Short contact (20 ms) | Second VB | 3.6 J | −3.89 (1.20) | −2.41 (0.62) | 0.002* | 4.81 (1.31) | 3.17 (1.07) | 0.003* | 8.70 (2.39) | 5.58 (1.52) | 0.003* |
| | | 6.0 J | −4.65 (1.32) | −3.00 (0.81) | 0.002* | 5.68 (1.28) | 3.88 (1.52) | 0.011* | 10.33 (2.17) | 6.88 (2.22) | 0.002* |
| | | 8.4 J | −5.35 (1.53) | −3.59 (0.90) | 0.002* | 6.21 (1.29) | 4.41 (1.74) | 0.028* | 11.56 (2.07) | 8.03 (2.53) | 0.003* |
| | | P-value | < 0.001* | < 0.001* | | 0.005* | 0.006* | | < 0.001* | < 0.001* | |
| | Third VB | 3.6 J | −2.64 (0.71) | −2.07 (0.82) | 0.046 | 3.45 (1.24) | 3.14 (1.37) | 0.306 | 6.09 (1.89) | 5.21 (2.16) | 0.342 |
| | | 6.0 J | −3.27 (0.74) | −2.63 (0.97) | 0.039 | 4.33 (1.40) | 3.99(1.65) | 0.415 | 7.56 (2.03) | 6.63 (2.59) | 0.384 |
| | | 8.4 J | −3.72 (0.79) | −3.14 (1.09) | 0.062 | 5.02 (1.56) | 4.68 (1.83) | 0.527 | 8.74 (2.23) | 7.81 (2.82) | 0.426 |
| | | P-value | < 0.001* | < 0.001* | | < 0.001* | < 0.001* | | < 0.001* | < 0.001* | |
| Long contact (40 ms) | Second VB | 3.6 J | −1.13 (0.63) | −0.63 (0.16) | 0.026 | 1.17 (0.82) | 0.70 (0.33) | 0.077 | 2.29 (1.41) | 1.33 (0.37) | 0.050* |
| | | 6.0 J | −1.49 (0.72) | −0.88 (0.26) | 0.023 | 1.51 (0.99) | 0.92 (0.49) | 0.054 | 2.99 (1.63) | 1.82 (0.50) | 0.043* |
| | | 8.4 J | −1.79 (0.70) | −1.03 (0.25) | 0.006 | 1.74 (1.00) | 1.02 (0.58) | 0.024 | 3.53 (1.63) | 2.10 (0.56) | 0.017* |
| | | P-value | < 0.001* | < 0.001* | | < 0.001* | < 0.001* | | < 0.001* | < 0.001* | |
| | Third VB | 3.6 J | −0.63 (0.17) | −0.56 (0.20) | 0.356 | 0.77 (0.24) | 0.65 (0.27) | 0.255 | 1.40 (0.31) | 1.21 (0.45) | 0.303 |
| | | 6.0 J | −0.94 (0.21) | −0.80 (0.20) | 0.120 | 1.02 (0.33) | 0.91 (0.31) | 0.265 | 1.97 (0.49) | 1.71 (0.47) | 0.250 |
| | | 8.4 J | −1.14 (0.23) | −0.98 (0.23) | 0.024 | 1.24 (0.48) | 1.03 (0.42) | 0.207 | 2.39 (0.65) | 2.07 (0.58) | 0.263 |
| | | P-value | < 0.001* | < 0.001* | | < 0.001* | < 0.001* | | < 0.001* | < 0.001* | |

Data are Average (Standard Deviation). Significance of comparison of short contact with respect to the long contact of all conditions were $p < 0.001$.

* Significant different between two groups



https://doi.org/10.1017/jmech.2011.2 Published online by Cambridge University Press

Table 2B The Outcomes of Acceleration Attenuation (AA) pre and post Fatigue at Different Levels of Contact Period and Impact Energy

| | Energy | Pre fatigue | Post fatigue | P-value (Fatigue) |
|---|---|---|---|---|
| Short contact (20 msec) | 3.6 J | 0.78 (0.18) | 1.05 (0.30) | 0.010* |
| | 6.0 J | 0.81 (0.20) | 1.09 (0.27) | 0.001* |
| | 8.4 J | 0.82 (0.19) | 1.08 (0.26) | 0.001* |
| | P-value (Energy) | 0.036* | 0.477 | |
| | Average | 0.81 (0.18) | 1.07 (0.27) | < 0.001* |
| Long contact (40 msec) | 3.6 J | 0.74 (0.32) | 0.96 (0.43) | 0.026* |
| | 6.0 J | 0.78 (0.33) | 1.00 (0.41) | 0.024* |
| | 8.4 J | 0.78 (0.33) | 1.04 (0.37) | 0.004* |
| | P-value (Energy) | 0.350 | 0.207 | |
| | Average | 0.77 (0.32) | 1.00 (0.39) | < 0.001* |
| Short vs. Long contact | P-value (Contact Period) | 0.585 | 0.425 | |
| | Average | 0.78 (0.260) | 1.04 (0.336) | < 0.001* |

Data are Average (Standard Deviation). * Significant different between two groups

Table 3A The Outcomes of the maximum input force and output force of 3-unit-motion-segment specimen Pre and Post Fatigue at Different Levels of Contact Period and Impact Energy

| | | | Input force (N) | | | Output force (N) | |
|---|---|---|---|---|---|---|---|
| | Energy | Pre fatigue | Post fatigue | P-value | Pre fatigue | Post fatigue | *P-value* |
| Short contact (20 msec) | 3.6 J | 1660 (119) | 1760 (97) | 0.009* | 2083 (174) | 2041 (154) | 0.222 |
| | 6.0 J | 2228 (121) | 2319 (123) | 0.026* | 2741 (215) | 2663 (191) | 0.114 |
| | 8.4 J | 2647 (181) | 2780 (138) | 0.030* | 3233 (263) | 3180 (216) | 0.348 |
| | P-value | < 0.001* | < 0.001* | | < 0.001* | < 0.001* | |
| Long contact (40 msec) | 3.6 J | 950 (48) | 951 (39) | 0.959 | 939 (57) | 918 (42) | 0.284 |
| | 6.0 J | 1245 (42) | 1269 (40) | 0.159 | 1223 (76) | 1231 (58) | 0.753 |
| | 8.4 J | 1520 (41) | 1558 (44) | 0.041* | 1492 (80) | 1511 (69) | 0.374 |
| | P-value | < 0.001* | < 0.001* | | < 0.001* | < 0.001* | |

Data are Average (Standard Deviation). Significance of comparison of short contact with respect to the long contact of all conditions were $p < 0.001$.
* Significant different between two groups

Table 3B The Outcomes of Ratio of Force Transmissibility (FT) pre and post Fatigue at Different Levels of Contact Period and Impact Energy

| | Energy | Pre fatigue | Post fatigue | P-value (Fatigue) |
|---|---|---|---|---|
| Short contact (20 msec) | 3.6 J | 1.26 (0.09) | 1.16 (0.04) | 0.001* |
| | 6.0 J | 1.24 (0.09) | 1.15 (0.04) | 0.002* |
| | 8.4 J | 1.23 (0.10) | 1.14 (0.04) | 0.005* |
| | P-value (Energy) | 0.016* | 0.003* | |
| | Average | 1.24 (0.09) | 1.15 (0.04) | < 0.001* |
| Long contact (40 msec) | 3.6 J | 0.98 (0.05) | 0.96 (0.03) | 0.204 |
| | 6.0 J | 0.98 (0.05) | 0.97 (0.04) | 0.466 |
| | 8.4 J | 0.96 (0.05) | 0.97 (0.04) | 0.573 |
| | P-value (Energy) | 0.391 | 0.361 | |
| | Average | 0.98 (0.05) | 0.97 (0.04) | 0.106 |
| Short vs. Long Contact | P-value (Contact Period) | < 0.001* | < 0.001* | |

Data are Average (Standard Deviation). * Significant different between two groups

### 3.4 Phase Delay of Force (PDF)

The time span and time to maximum forces during short contact loading decreased post fatigue (Table 4A). The PDF did not change post fatigue. The PDF was independent of impact energy pre and post fatigue. The PDF decreased with contact period pre fatigue. The PDF did not change with contact period post fatigue (Table 4B).

## 4. DISCUSSION

The outcome of biological structure, *e.g.*, spine, post fatigue loading was complicated and difficult to compare among different researches. It was because the type and magnitude of fatigue loading was not clearly defined and the loading conditions were not consistent. In the test of engineering materials, the fatigue test was



https://doi.org/10.1017/jmech.2011.2 Published online by Cambridge University Press

Table 4A The Outcomes of the time span and time to maximum input and output force of 3-unit-motion-segment specimen Pre and Post Fatigue at Different Levels of Contact Period and Impact Energy

| | | T_span_input (ms) | | | T_span_output (ms) | | |
|---|---|---|---|---|---|---|---|
| | Energy | Pre fatigue | Post fatigue | P-value | Pre fatigue | Post fatigue | P-value |
| Short contact (20 msec) | 3.6 J | 19.7 (2.3) | 18.7 (1.8) | 0.002* | 18.2 (2.2) | 16.9 (1.7) | 0.004* |
| | 6.0 J | 18.7 (2.3) | 17.9 (2.0) | 0.004* | 18.0 (2.3) | 16.9 (1.8) | 0.003* |
| | 8.4 J | 18.3 (2.4) | 17.4 (2.0) | 0.002* | 17.4 (2.5) | 16.5 (1.6) | 0.042* |
| | P-value | < 0.001* | < 0.001* | | 0.185 | 0.300 | |
| Long contact (40 msec) | 3.6 J | 43.8 (3.1) | 42.3 (1.3) | 0.129 | 38.8 (4.0) | 37.8 (3.9) | 0.618 |
| | 6.0 J | 39.2 (1.2) | 38.5 (0.9) | 0.203 | 34.5 (1.3) | 33.8 (1.4) | 0.239 |
| | 8.4 J | 37.3 (1.1) | 36.5 (0.9) | 0.083 | 32.9 (0.6) | 32.5 (1.1) | 0.169 |
| | P-value | 0.001* | < 0.001* | | 0.004* | 0.005* | |
| | | T_max_input (ms) | | | T_max_output (ms) | | |
| | Energy | Pre fatigue | Post fatigue | P-value | Pre fatigue | Post fatigue | P-value |
| Short contact (20 msec) | 3.6 J | 8.7 (1.0) | 8.29 (0.9) | 0.022* | 9.2 (0.6) | 8.8 (0.4) | 0.027* |
| | 6.0 J | 8.4 (0.9) | 8.05 (0.8) | 0.020* | 8.9 (0.5) | 8.6 (0.4) | 0.028* |
| | 8.4 J | 8.2 (0.8) | 7.89 (0.7) | 0.023* | 8.8 (0.5) | 8.5 (0.4) | 0.024* |
| | P-value | < 0.001* | < 0.001* | | < 0.001* | 0.004* | |
| Long contact (40 msec) | 3.6 J | 18.8 (0.5) | 18.7 (0.5) | 0.740 | 18.6 (2.8) | 20.0 (1.6) | 0.236 |
| | 6.0 J | 17.3 (0.6) | 17.2 (0.3) | 0.783 | 17.1 (2.8) | 18.0 (1.4) | 0.522 |
| | 8.4 J | 17.6 (3.1) | 16.4 (0.3) | 0.326 | 17.8 (3.4) | 16.9 (1.0) | 0.487 |
| | P-value | 0.289 | < 0.001* | | 0.355 | < 0.001* | |

Data are Average (Standard Deviation). Significance of comparison of short contact with respect to the long contact of all conditions were $p < 0.001$.
* Significant different between two groups

Table 4B The Outcomes of Phase Delay of Force (PDF, %) pre and post Fatigue at Different Levels of Contact Period and Impact Energy

| | Energy | Pre fatigue | Post fatigue | P-value (Fatigue) |
|---|---|---|---|---|
| Short contact (20 msec) | 3.6 J | 2.5% (2.4%) | 2.6% (3.6%) | 0.923 |
| | 6.0 J | 2.8% (1.9%) | 2.8% (3.0%) | 0.931 |
| | 8.4 J | 3.3% (2.1%) | 3.3% (3.1%) | 0.946 |
| | P-value (Energy) | 0.064 | 0.417 | |
| | Average | 2.9% (2.1%) | 2.9% (3.1%) | 0.982 |
| Long contact (40 msec) | 3.6 J | –0.3% (6.7%) | 3.1% (4.2%) | 0.259 |
| | 6.0 J | –0.5% (6.0%) | 2.0% (3.5%) | 0.442 |
| | 8.4 J | 0.4% (5.4%) | 1.4% (2.5%) | 0.612 |
| | P-value (Energy) | 0.918 | 0.223 | |
| | Average | –0.1% (5.8%) | 2.2% (3.4%) | 0.129 |
| Short vs. Long Contact | P-value (Contact Period) | 0.026* | 0.544 | |

Data are Average (Standard Deviation). * Significant different between two groups

categorized into two major types, *i.e.*, the high cycle fatigue and the low cycle fatigue. The high cycle fatigue was classified as high number cycle with mild loading magnitude, and the number of high cycle fatigue test was usually up to 1 million cycles. In the study of spine biomechanics, there is less discussion about the differentiation between the high cycle and low cycle fatigue loading. The fatigue loading can be distinguished into these categories by the activities that spine may encountered. For example, the low cycle fatigue may simulate the loading during repetitive lifting from moderate to heavy weight (3Nm for 9,000 cycles [19], 500N to 3150N, for 8253, 3257 and 263 cycles at 0, 22.5, and 45 degree flexion [20,21], 1,472N (mean) for 6,000 cycles [17], and 3,076N (mean) for 9,600 cycles [22]). The high cycle fatigue may simulate the loading during a vibratory environment without excessive bearing (260N (mean) for 86,400 cycles [23]). The loading magnitude of 425N (mean) for 90,000 cycles used in current study belongs to the high cycle fatigue loading condition. Differentiation of fatigue loading helps the implementation of experimental results.

The limitation of current protocol should be noted.



https://doi.org/10.1017/jmech.2011.2 Published online by Cambridge University Press

The natural re-hydration process was not simulated in this study. Mechanical loading of the intervertebral disc generate high magnitudes of fluid and osmotic pressures; this results in the interstitial fluid loss and may contribute to tissue fail, *e.g.*, AF tears, that may link to the decrease of disc height, fluid pressure and disc stiffness [24]. In this study, the disc fluid was squeezed out and the AF was injured post fatigue loading. These two factors both affect mechanical property of disc. Since the disc re-hydrated during an in vivo vibratory loading condition, the current results may represent the worst scenario that the disc may encounter [25,26]. Therefore, the mechanism and contributions of these two factors to the disc shock absorption capability may need further investigation.

The impact energy of this study ranged from 3.6 J to 8.4 J. The corresponding resultant force ranged from 1,700N to 3,200N during short contact loading and from 950N to 1,500N during long contact loading. The peak compressive load of the spine was greater than 8,600N in blocking maneuvers in football linemen [27], 17,000N in weight lifters [28], and 5,500N in tricked fall [29]. The loading condition of current study could simulate medium to high loading, but not to the extreme loading yet.

The loading axis of the quadruped spine was mainly along its long axis, just like human spine [30]. The porcine spine is analogue to human spine in terms of anatomic, geometric and functional characteristics [23,31,32]. However, limitations of using the porcine spine should be addressed. First, the current study applied vertical loading along the long axis of motion segment. The anterior porcine facet joint, which is analogous to the superior facet joint in human spine, is a hook-like process and the human facet joint is a straight process. This geometric difference should significantly increase the load sharing percentage of facet joint during anteroposterior and lateral shear loading, but less in the axial direction. Secondly, the specimens were harvested from 6 month old swine, of which the physiological condition is close to the one of young human adult. Therefore, the results of current study should be limited to the healthy disc, but not the degenerated disc.

The AA was expressed as original ratio instead of dB unit for the benefit of intuitive interpretation in this study; however, the dB unit was the convention that used for the measurement and comparison of shock attenuation by most engineers. The AA of a single disc found in this study was −1.06dB (original ratio = 0.78) pre fatigue and 0.14dB (original ratio = 1.04) post fatigue. The AA of the sacrum (output) with respect to the shank (input) during running was from −3dB (decline running) to −8dB (level running, estimated by the graph) [33]. The AA of the head (output) with respect to the shank (input) during an impact to the foot was from −6dB (soft surface) to −7dB (hard surface, calculated by the table) [34]. Our data showed that the AA of an intact disc was −1.06dB. Theoretically, seven serial discs in line can attenuate the acceleration for −7dB. However, with the complex structure of human body and spinal column, the disc may not attenuate the acceleration at its maximum efficiency during in vivo loading. During the in vivo impact loading condition, the absolute value of AA of disc may be less than −1.06dB.

We used PDF to describe the phase distortion of force transmission in this study. Traditionally, the phase angle was used to describe the phase distortion of a structure during vibration. For example, the phase angle of disc prosthesis during vibration was reported to be 10 degree (close to 2.8% using our definition) [35]. The theoretical formulation of phase distortion due to impact and vibration may not be the same. Before the theoretical formulation of disc during impact loading was developed, the phenomenological shock response of motion segment was archived using the PDF. These data may be helpful in the future for the validation of theoretical impact simulation of motion segment.

The energy transmission of the spinal column can be characterized by the capability of the shock absorption and vibrations [34]. The long term fatigue loading was know to injury the AF; hence affect the disc dynamic properties such as stiffness and damping coefficient [36]. In this study, we directly evaluated the disc dynamic changes such as AA, FT, and PDF for an intuitive comparison. The AA is a factor to examine the shock absorption capacity of disc. Previous studies showed that changes of intradiscal pressure will lead to different AA [34,37]. We found the AA increased post fatigue loading which may be due to the less viscosity of motion segment. The less viscosity of motion segment may be due to the loss of water post fatigue loading. The FT can be used to quantify the shock absorption of disc [35]. The higher FT indicates higher internal force. The FT was found to be significantly higher than 1 during the short contact period, but not in the long contact period. This phenomenon may indicate that the internal force of disc is higher during short contact time. The PDF is indeed still an engineering index to measure the hysteresis of a viscoelastic damping system. The presentation of PDF here may be helpful for the designing of new disc prosthesis to come [38]. We found the PDF is invariant of fatigue loading, impact energy and contact time, which may be a good news for the design of new disc prosthesis.

Several tasks may be worthy of trying in the near future. First, the short-term viscoelastic or poroelastic material properties of disc can be estimated by the theoretical analysis of disc using the results of current study. Second, we did not know if the fatigue loading of this study creates permanent injury. The in vitro biomechanical experiments showed both the reversible [39] and irreversible [40] changes of disc mechanical properties post repetitive loading. In the future, establishing the index of critical fatigue loading is imperative for preventing permanent injury of disc.

In summary, this study showed that the fatigue loading decreased the shock attenuation of disc and motion segment. The AA of disc was invariant of impact energy and contact period, but decreased post fatigue. The AA is a good index to evaluate the degree of disc fatigue injury.



https://doi.org/10.1017/jmech.2011.2 Published online by Cambridge University Press

## REFERENCES


1. Marras, W. S., Lavender, S. A., Leurgans, S. E., Fathallah, F. A., Ferguson, S. A., Allread, W. G. and Rajulu, S. L., "Biomechanical Risk Factors for Occupationally Related Low Back Disorders," *Ergonomics*, **38**, pp. 377–410 (1995).
2. Marras, W. S., Parakkat, J., Chany, A. M., Yang, G., Burr, D. and Lavender, S. A., "Spine Loading as a Function of Lift Frequency, Exposure Duration, and Work Experience," *Clinical Biomechanics*, **21**, pp. 345–352 (2006).
3. Kumar, S., "Cumulative Load as a Risk Factor for Back Pain," *Spine*, **15**, pp. 1311–1316 (1990).
4. Wilder, D. G. and Pope, M. H., "Epidemiological and Aetiological Aspects of Low Back Pain in Vibration Environments—An Update," *Clinical Biomechanics*, **11**, pp. 61–73 (1996).
5. Kumar, A., Varghese, M., Mohan, D., Mahajan, P., Gulati, P. and Kale, S., "Effect of Whole-Body Vibration on the Low Back. A Study of Tractor-Driving Farmers in North India," *Spine*, **24**, pp. 2506–2515 (1999).
6. Althoff, I., Brinckmann, P., Frobin, W., Sandover, J. and Burton, K., "An Improved Method of Stature Measurement for Quantitative Determination of Spinal Loading. Application to Sitting Postures and Whole Body Vibration," *Spine*, **17**, pp. 682–693 (1992).
7. Burton, A. K. and Sandover, J., "Back Pain in Grand Prix Drivers: A 'Found' Experiment," *Applied Ergonomics*, **18**, pp. 3–8 (1987).
8. Pope, M. H., Wilder, D. G., Jorneus, L., Broman, H., Svensson, M. and Andersson, G., "The Response of the Seated Human to Sinusoidal Vibration and Impact," *Journal of Biomechanical Engneering*, **109**, pp. 279–284 (1987).
9. Lee, C. K., Kim, Y. E., Lee, C. S., Hong, Y. M., Jung, J. M. and Goel, V. K., "Impact Response of the Intervertebral Disc in a Finite-Element Model," *Spine*, **25**, pp. 2431–2439 (2000).
10. Lee, C. K. and Goel, V. K., "Artificial Disc Prosthesis: Design Concepts and Criteria," *The Spine Journal*, **4**, pp. 209S–218S (2004).
11. Taksali, S., Grauer, J. N. and Vaccaro, A. R., "Material Considerations for Intervertebral Disc Replacement Implants," *The Spine Journal*, **4**, pp. 231S–238S (2004).
12. Valdevit, A. and Errico, T. J., "Design and Evaluation of the Flexicore Metal-On-Metal Intervertebral Disc Prosthesis," *The Spine Journal*, **4**, pp. 276S–288S (2004).
13. Galante, J. O., "Tensile Properties of the Human Lumbar Annulus Fibrosus," *Acta Orthopaedica Scandinavica*, pp. Suppl 100:1–91 (1967).
14. Chanchairujira, K., Chung, C. B., Kim, J. Y., Papakonstantinou, O., Lee, M. H., Clopton, P. and Resnick, D., "Intervertebral Disk Calcification of the Spine in an Elderly Population: Radiographic Prevalence, Location, and Distribution and Correlation with Spinal Degeneration," *Radiology*, **230**, pp. 499–503 (2004).
15. Panjabi, M. M., Takata, K., Goel, V., Federico, D., Oxland, T., Duranceau, J. and Krag, M., "Thoracic Human Vertebrae. Quantitative Three-Dimensional Anatomy," *Spine*, **16**, pp. 888–901 (1991).
16. Wang, J. L. and Lee, Y. L., "The shock Attenuation Properties of Straight Standing Knee Joint Using Different Shock Absorbers and Energy Input.," *Ournal of the Chinese Institute of Engineers*, **26**, pp. 729–736 (2003).
17. Aultman, C. D., Scannell, J. and McGill, S. M., "The Direction of Progressive Herniation in Porcine Spine Motion Segments is Influenced by the Orientation of the Bending Axis," *Clinical Biomechanics*, **20**, pp. 126–129 (2005).
18. Adams, M. A. and Hutton, W. C., "Gradual Disc Prolapse," *Spine*, **10**, pp. 524–531 (1985).
19. Goel, V. K., Voo, L. M., Weinstein, J. N., Liu, Y. K., Okuma, T. and Njus, G. O., "Response of the Ligamentous Lumbar Spine to Cyclic Bending Loads," *Spine*, **13**, pp. 294–300 (1988).
20. Gallagher, S., Marras, W. S., Litsky, A. S. and Burr, D., "An Exploratory Study of Loading and Morphometric Factors Associated with Specific Failure Modes in Fatigue Testing of Lumbar Motion Segments," *Clinical Biomechanics*, **21**, pp. 228–234 (2006).
21. Gallagher, S., Marras, W. S., Litsky, A. S. and Burr, D., "Torso Flexion Loads and the Fatigue Failure of Human Lumbosacral Motion Segments," *Spine*, **30**, pp. 2265–2273 (2005).
22. Adams, M. A. and Hutton, W. C., "The Effect of Fatigue on the Lumbar Intervertebral Disc," *Journal of Bone and Joint Surgery, British Volume*, **65**, pp. 199–203 (1983).
23. Callaghan, J. P. and McGill, S. M., "Intervertebral Disc Herniation: Studies on a Porcine Model Exposed to Highly Repetitive Flexion/Extension Motion with Compressive Force," *Clinical Biomechanics*, **16**, pp. 28–37 (2001).
24. Setton, L. A. and Chen, J., "Mechanobiology of the Intervertebral Disc and Relevance to Disc Degeneration," *Journal of Bone and Joint Surgery, American Volume*, 88 Suppl 2, pp. 52–57 (2006).
25. Natarajan, R. N., Williams, J. R. and Andersson, G. B., "Recent Advances in Analytical Modeling of Lumbar Disc Degeneration," *Spine*, **29**, pp. 2733–2741 (2004).
26. Masuoka, K., Michalek, A. J., MacLean, J. J., Stokes, I. A. and Iatridis, J. C., "Different Effects of Static Versus Cyclic Compressive Loading on Rat Intervertebral Disc Height and Water Loss in Vitro," *Spine*, **32**, pp. 1974–1979 (2007).
27. Gatt, C. J., Jr., Hosea, T. M., Palumbo, R. C. and Zawadsky, J. P., "Impact Loading of the Lumbar Spine During Football Blocking," *The American Journal of Sports Medicine*, **25**, pp. 317–321 (1997).
28. Cholewicki, J., McGill, S. M. and Norman, R. W., "Lumbar Spine Loads During the Lifting of Extremely Heavy Weights," *Medicine & Science in Sports & Exercise*, **23**, pp. 1179–1186 (1991).
29. Essendrop, M., Trojel Hye-Knudsen, C., Skotte, J.,




https://doi.org/10.1017/jmech.2011.2 Published online by Cambridge University Press

Faber Hansen, A. and Schibye, B., "Fast Development of High Intra-Abdominal Pressure When a Trained Participant is Exposed to Heavy, Sudden Trunk Loads," *Spine*, **29**, pp. 94–99 (2004).
30. Smit, T. H., "The Use of a Quadruped as an in Vivo Model for the Study of the Spine—Biomechanical Considerations," *European Spine Journal*, **11**, pp. 137–144 (2002).
31. McLain, R. F., Yerby, S. A. and Moseley, T. A., "Comparative Morphometry of L4 Vertebrae: Comparison of Large Animal Models for the Human Lumbar Spine," *Spine*, **27**, pp. E200–E206 (2002).
32. Cheng, C. H., Chen, T. Y., Kuo, Y. W. and Wang, J. L., "The Mechanics of Cervical Muscle Recruitment on Cervical Spine Stability—A Biomechanical in Vitro Study Using Porcine Model," *Journal of Mechanics*, **24**, pp. 63–68 (2008).
33. Mizrahi, J., Verbitsky, O. and Isakov, E., "Shock Accelerations and Attenuation in Downhill and Level Running," *Clinical Biomechanics*, **15**, pp. 15–20 (2000).
34. Lafortune, M. A., Lake, M. J. and Hennig, E. M., "Differential Shock Transmission Response of the Human Body to Impact Severity and Lower Limb Posture," *Journal of Biomechanics*, **29**, pp. 1531–1537 (1996).
35. LeHuec, J. C., Kiaer, T., Friesem, T., Mathews, H., Liu, M. and Eisermann, L., "Shock Absorption in Lumbar Disc Prosthesis: A Preliminary Mechanical Study," *Journal of Spinal Disorders & Techniques*, **16**, pp. 346–351 (2003).
36. Wang, J. L., Wu, T. K., Lin, T. C., Cheng, C. H. and Huang, S. C., "Rest Cannot Always Recover the Dynamic Properties of Fatigue-Loaded Intervertebral Disc," *Spine*, **33**, pp. 1863–1869 (2008).
37. Helliwell, P. S., Smeathers, J. E. and Wright, V., "Shock Absorption by the Spinal Column in Normals and in Ankylosing Spondylitis," *Proceedings of the Institution of Mechanical Engineers. Part H, Journal of engineering in medicine*, **203**, pp. 187–190 (1989).
38. Smeathers, J. E., "Transient Vibrations Caused by Heel Strike," *Proceedings of the Institution of Mechanical Engineers. Part H, Journal of engineering in medicine*, **203**, pp. 181–186 (1989).
39. Johannessen, W., Vresilovic, E. J., Wright, A. C. and Elliott, D. M., "Intervertebral Disc Mechanics are Restored Following Cyclic Loading and Unloaded Recovery," *Annals of Biomedical Engineering*, **32**, pp. 70–76 (2004).
40. van der Veen, A. J., Mullender, M., Smit, T. H., Kingma, I. and van Dieen, J. H., "Flow-Related Mechanics of the Intervertebral Disc: The Validity of an in Vitro Model," *Spine*, **30**, pp. E534–E539 (2005).

(Manuscript received November 20, 2009,
accepted for publication April 9, 2010.)



https://doi.org/10.1017/jmech.2011.2 Published online by Cambridge University Press